Astronomy & Astrophysics manuscript no. ms
January 29, 2019

Transient processing and analysis using AMPEL: Alert Management, Photometry and Evaluation of Lightcurves

J. Nordin[1], V. Brinnel[1], J. van Santen[2], M. Bulla[3], U. Feindt[3], A. Franckowiak[2], M. Giomi[1], M. Kowalski[1,2], N. Miranda[1], L. Rauch[2], M. Rigault[3], R. Stein[2], and ...

[1] Institute of Physics, Humboldt-Universität zu Berlin, Newtonstr. 15, 12489 Berlin, Germany
[2] Deutsches Elektronen-Synchrotron, D-15735 Zeuthen, Germany
[3] The Oskar Klein Centre, Department of Physics, Stockholm University, AlbaNova, SE-106 91 Stockholm, Sweden Université de Lyon, F-69622, Lyon, France; Université de Lyon 1, Villeurbanne; CNRS/IN2P3, Institut de Physique Nucléaire de Lyon.

January 29, 2019

ABSTRACT

Both multi-messenger astronomy and new high-throughput surveys require the development of flexible tools for the selection and analysis of astrophysical transients. We here introduce the Alert Management, Photometry and Evaluation of Lightcurves (AMPEL) system, a streaming data analysis framework. AMPEL incorporates, but is not limited to, an alert broker, coupling it with the capability to host user contributed code to analyze and react to events. These tools are embedded into a framework that encourages provenance and keeps track of the varying information states that a transient displays. The latter concept includes information gathered over time, but also tracks varying data access levels and e.g. improved calibration. Taken together, AMPEL provides a tool that can assist in filtering transients in real time, running realistic alert reaction simulations, reprocessing of full datasets as well as the final scientific analysis of transient data. To demonstrate AMPEL we reprocess the first four first months of Zwicky Transient Facility (ZTF) public alerts. Using more than 200 different transient selection functions, we compare their yield with all confirmed Type Ia supernovae reported to the Transient Name Server (TNS). We confirm ZTF completeness with all candidates falling on active CCD regions being detected. This incudes those transients that were originally reported by other surveys. Based on this exploration, we introduce the criteria upon which AMPEL submits high quality extragalactic supernova candidates from ZTF to the TNS in real-time. We further describe the AMPEL live multi-messenger correlation between ZTF data and IceCube neutrino alerts. This text also introduces how users can design their own channels for inclusion in the AMPEL live instance that parses the ZTF stream.

1. Introduction

Transient astronomy has traditionally used optical telescopes to detect variable objects, both within and beyond our galaxy, with a peak sensitivity for events that vary on timescales of a week. This field has now entered a new phase in which multi-messenger astronomy allows for near real-time detection of transients through correlations between observations of different messengers. The initial report of GW170817 from LIGO/VIRGO, and the subsequent search and detection of an X-ray/optical counterpart, provides a first, inspiring example of this (Abbott et al. 2017). Shortly after, the observation of a flaring blazar coincident with a high-energy neutrino detected by IceCube illustrated again the scientific potential of time domain multi-messenger astronomy (IceCube Collaboration et al. 2018). Optical surveys now observe the full sky daily, to a depth which encompasses both distant, bright objects and nearby, faint ones. We can thus simultaneously find rare objects, obtain an accounting of the variable Universe, and probe fundamental physics at scales beyong the reach of terrestrial accelerators. Exploiting these opportunities is currently constrained as much by software and method development as by available instruments (Allen et al. 2018).

The plans for the Large Synoptic Survey Telescope (LSST) provides a sample scale for high-rate transient discovery. LSST is expected to scan large regions of the sky to great depth, with sufficient cadence for more than 10^6 astrophysical transients to be discovered each night. Each such detection will be immediately streamed to the community as an *alert*. The challenge of distributing this information for real-time follow-up observations is to be solved through a set of *brokers*, which will receive the full data flow and allow end-users to select the small subset that merits further study (Jurić et al. 2017). One example is the Arizona-NOAO Temporal Analysis and Response to Events System (ANTARES), which provides a system for real-time characterization and annotation of alerts before they are relayed further downstream (Saha et al. 2014). Earlier systems for transient information distribution include the Gamma-ray Coordinates Network and the more general Astronomer's Telegram. Other recent developments include the Astrophysical Multimessenger Observatory Network (AMON), which provides a framework real-time correlation of transient data streams from different high-energy observatories, and the Transient Name Server (TNS), which maintains the current IAU repository for potential and confirmed extragalactic transients (Smith et al. 2013).

While LSST will come online only in 2022, the Zwicky Transient Facility (ZTF) has been operating since March 2018. ZTF employs a wide-field camera mounted on the Palomar P48 telescope, and is capable of scanning more than 3750 square degrees to a depth of 20.5 mag each hour (Bellm et al. 2019). This makes ZTF a wider, shallower precursor to LSST, with a depth more suited

to spectroscopic follow-up observations. ZTF observations are immediately transferred to the IPAC data center for reprocessing and image subtraction. Any significant point source-like residual flux in the subtracted image triggers the creation of an alert. Alerts are serialized and distributed through a Kafka[1] server hosted at the DiRAC centre at University of Washington (Patterson et al. 2019). Each alert contains primary properties like position and brightness, but also ancillary detection information and higher-level derived values such as the RealBogus score which aims to distinguish real detections from image artifacts. Full details on the reduction pipeline and alert content can be found in Masci et al. (2019), while an overview of the information distribution can be found in the top row of Fig. 1.

We here present `AMPEL` (Alert Management, Photometry and Evaluation of Lightcurves) as a tool to accept, process and react to streams of transient data. `AMPEL` contains a broker as the first of four pipeline levels, or 'tiers', but complements this with a framework enabling analysis methods to be easily and consistently applied to large data volumes. The same set of input data can be repeatedly reprocessed with progressively refined analysis software, while the same algorithms can thhen also be applied to real-time, archived and simulated data samples. Analysis and reaction methods can be contributed through the implementation of simple `python` classes, ensuring compatability with the vast majority of current community tools to be used. `AMPEL` functions as a public broker for use with the public ZTF alert stream, meaning that community members can provide analysis modules for inclusion the real-time data processing.

This paper is structured as follows: `AMPEL` requirements are first described in section 2, after which the design concepts are presented in Sec. 3, some specific implementation choices detailed in Sec. 4 and instructions for using `AMPEL` are provided in Sec. 5. In Sec. 6 we discuss two sample `AMPEL` uses: systematic reprocessing of archived alerts to investigate transient search completeness and efficiency, and live multi-messenger matching between optical and neutrino data-streams. The discussion (Sec. 7) introduces the automatic `AMPEL` submission of high-quality extragalactic astronomical transients to the TNS, from which astronomers can immediately find potential supernova or AGN variables without having to do any broker configuration. The material presented here focuses on the design and concepts of `AMPEL`, and acts as a complement to the software design tools contained in the `AMPEL` sample repository.[2]

2. Requirements

Guided by an overarching goal of analysing data streams, we here lay out the corresponding design requirements that have shaped `AMPEL` developement:

Provenance and reproducibility: Data provenance ecapsulates the philosophy that the origin and manipulation of a dataset should be easily traceable. As data volumes grow, and as astronomers increasingly seek to combine ever more diverse datasets, the concept of data provenance will be of central importance. In this era, individual scientists can be expected neither to master all details of a given workflow, nor to inspect all data by hand. As an alternative, these scientsts must instead rely on documentation accompanying the data. While provenance is a minimal requirement for such analysis, a more ambitious goal is *replayability*. Replaying an archival transient survey offline would involve providing a virtual survey in which the entire analysis chain is simulated, from transient detection to the evaluation of triggered follow-up observations. In essence, this amounts to answering the question: *If I had changed my search or follow-up parameters, what candidates would have been selected?* Because any given transient will only be observed once, replayability is as close to the standard scientific goal of reproducibility as astronomers can get.

Analysis flexibility: The next decades will see an unprecedented range of completementary surveys looking for transients through gravitational waves, neutrinos and multiwavelength photons. These will feed a sprawling community of diverse science interests. We would like a transient software framework that is sufficiently flexible to give full freedom inanalysis design, while still being compatible with existing tools and software.

Versions of data and software: It is typical that the value of a measurement evolves over time, from a preliminary real-time result to final published data. This is driven both by changes in the quantitative interpretation of the observations, as well as a progressive increase in analysis complexity. The first dimension involves changes such as improved calibration, while the second incorporates, for example, more computationally expensive studies only run on subsets of the data. So far it has been hard to study the full impact of incremental changes in these two dimensions, and how final results should be interpreted with respect to, for example, non-detections and varying instrument sensitivities. A related community challenge is to recognize, reference and motivate continued development of well-written software.

Alert rate: Current optical transient surveys such as DES, ZTF, ASAS-SN and ATLAS, as well as future ones (LSST), do or will provide tens of thousands to millions of detections each night. With such scale, it is impossible for human inspection of all candidates, even assuming that artifacts could be perfectly removed.[3] A simplistic solution to this problem is to only select a very small subset from the full stream, for example a handful of the *X* brightest objects, for which additional human inspection is feasible.

[1] https://kafka.apache.org

[2] https://github.com/AmpelProject/Ampel-contrib-sample

[3] For optical surveys, a majority of these "detections" are actually artifacts induced through the subtraction of a reference image. Machine learning techniques, such as RealBogus for ZTF, are increasingly powerful at separating these from real astronomical transients. However, this separation can never be perfect and any transient program has to weigh how aggressive to make use of these classifications.

A more complete approach would be based on retaining much larger sets of targets as part of the analysis, from which subsets are complemented with varying levels of follow-up information. As the initial subset selection will by neccesity be done in an automated streaming context, the accompanying analysis framework must be able to trace and model these real-time decisions.

3. AMPEL in a nutshell

AMPEL is a framework for analysing and reacting to streamed information, with a focus on astronomical transients. Fulfilling the above design goals requires a flexible framework built using a set of general concepts. These will be introduced in this section, accompanied by examples based on optical data from ZTF. A schematic of this process can be found in Fig. 1.

The core object in AMPEL is a *transient*, a single object identified by a creation date and a region of origin in the sky. Each transient is linked to a set of *datapoints* that represent individual measurements.[4] Datapoints can be added, updated, marked as bad, or replaced, but never removed. Each datapoint can be associated with flags indicating e.g. any masking or proprietary restrictions . Transients and datapoints are connected by *states*, where a state references a *compound* of datapoints. A state represents a view of a transient available at some time and for some observer. For an optical photometric survey, a compound can be directly interpreted as a set of flux measurements or a lightcurve.

Example: A ZTF alert corresponds to a potential transient. Datapoints here are simply the photometric magnitudes reported by ZTF. When first inserted, a transient has a single state with a compound consisting of the datapoints in the initial alert. If this transient is detected again, the new datapoint is added to the collection and a new state created containing both previous and new data. Should the first datapoint be public but the second datapoint be private, only users with proper access will see the updated state.

Using AMPEL means creating a *channel*, corresponding to a specific science goal, which prescribes behavior at four different stages, or *tiers*. What is to be done at each tier can be generally defined by answers to the questions: "Tier 0: *What are the minimal requirements for an alert to be interesting?*", "Tier 1: *How can observations evolve with time?*", "Tier 2: *What calculations should be done on each of the candidates states?*", "Tier 3: *What operations should be done at timed intervals?*"[5]

In Tier 0 (T0), the full alert stream is *filtered* to only include potentially interesting candidates. This tier thus works as a data broker, because objects that merit further study are selected from the incoming alert stream. However, unlike most brokers, accepted transients are nserted into a database (DB) of active transients rather than immediately being sent downstream. Users can either provide their own algorithm for filtering, or configure one of the public filter classes, according to their needs.

Example T0: The simple AMPEL *channel "BrightNStable" looks for variables with at least three detections within* 10 *days and at least one detection brighter than* 18 *mag. This is implemented through a* `python` *class that operates on an alert and returns* `True` *if all criteria are fulfilled.* AMPEL *will test every ZTF alert using this class, and all alerts that pass the cut are added to the active transient DB. The transient is there tagged with the "BrightNStable" ID.*

Tier 1 (T1) is largely autonomous and exists in parallel to the other tiers. T1 carries out duties related to *updates* of datapoints or states. Example activities include completingn transient states with datapoints that were present in new alerts but where these were not individually accepted by the channel filter (e.g., in the case of lower significance detections at late phases), as well as queringy an external archive for updated calibration.

Additional transient information is derived or retrieved in Tier 2 (T2), and are always connected to a state and stored as a *ScienceRecord*. T2 modules either apply to the empty state, relevant for e.g. catalog matching that only depends on the position, or applies to a state where it provides new properties derived from a specific compound. In the latter case, the T2 task will be called again as soon as a new state is created. This could be due both to new observations or, for example, updated calibration of old datapoints. Possible T2 modules include lightcurve fitting, photometric redshift estimation, machine learning classification, and catalog matching.

Example T2: For an optical transient, a state corresponds to a lightcurve and each photometric observation is represented by a datapoint. A new observation of the transient would extend the lightcurve and thus create a new state."BrightNStable" requests a third order polynomial fit for each state using the `T2PolyFit` *class. The outcome, in this case polynomial coefficients, are saved to the database.*

The final AMPEL level, Tier 3 (T3), consists of *schedulable* actions. While T2s are initiated by events (the addition of new states), T3 modules are executed at pre-determined times. These can range from yearly data dumps, to daily updates, to effectively real-time execution every few seconds. T3 processes access data through the *TransientView*, which concatenates all information regarding a transient. This includes both states and ScienceRecords that are accessible by the channel. T3s iterate through all transients of a channel. This allows for an evaluation of multiple ScienceRecords, and comparisons between different objects or, more generally, any kind of population analysis. One typical use cases is the ranking of candidates which would be interesting to observe on a given night. T3 modules include options to push and pull information from for example Slack, TNS and web-servers.

[4] Note that this is a many-to-many connection; multiple transients can be connected to the same datapoint due to e.g. positional uncertainty. Datapoints can also originate from different sources.

[5] Timed intervals include very high frequencies or effectively real-time response channels.

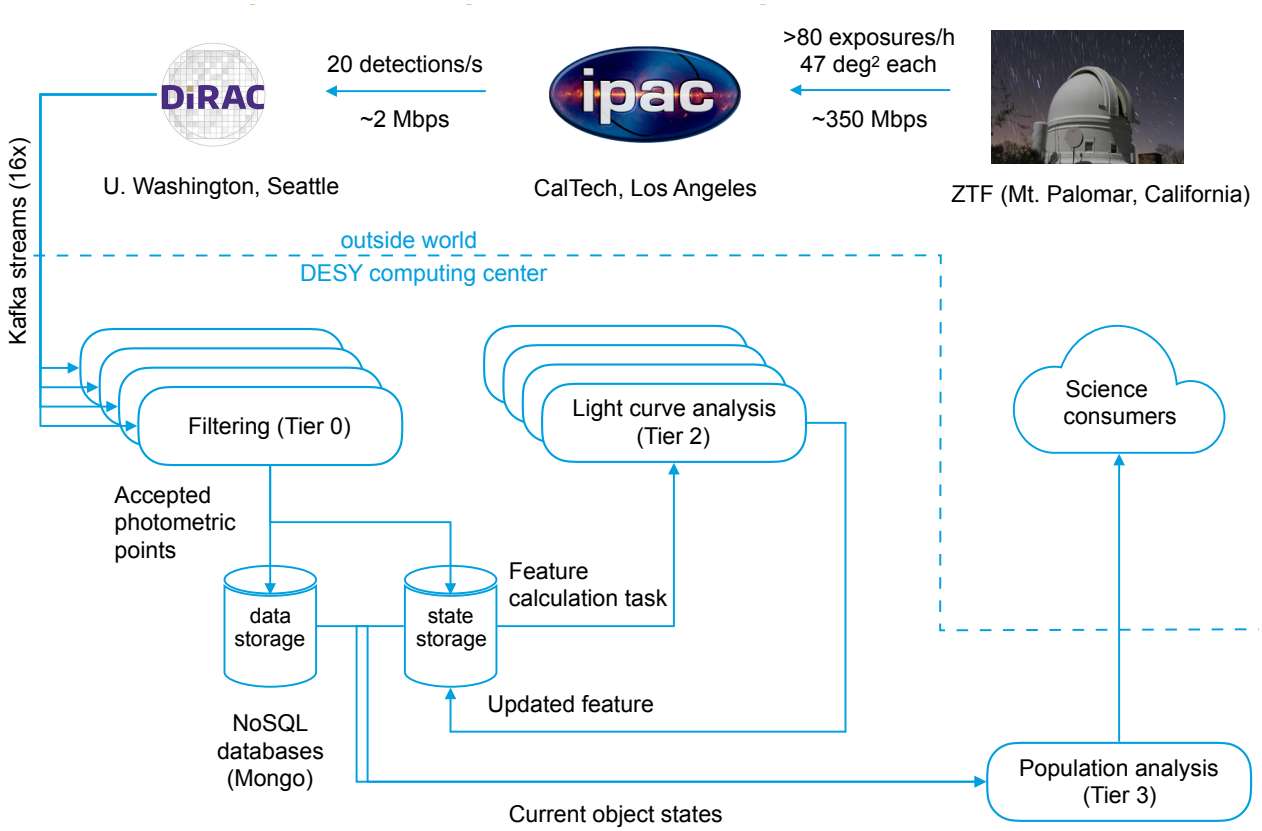

Fig. 1. AMPEL framework schematic. *Upper panels:* Summary of the ZTF alert distribution system. *Lower panels:* Sample AMPEL process: A set of parallel alert processors examine the incoming Kafka Stream (Tier 0). Accepted alert data is saved into a collection, while states are recorded in another. A light curve analysis (Tier 2) is performed on all states. The available data, including the Tier 2 output, is examined in a Tier 3 module which selects which transients should be passed on to Science consumers. This particular use case does not contain a Tier 1 stage.

Example T3: The science goal of "BrightNStable" is to observe transients with a steady rise. At the T3 stage the channel therefore loops through the TransientViews, and examines all T2PolyFit science records for fit parameters which indicates a lasting linear rise. Any transients fulfilling the final criteria trigger an immediate notification sent to the user. This test is scheduled to be performed at 13:15 UT each day.

4. Implementation

Based on the above requirements, and using the AMPEL concepts, we here expand on implementational aspects.

Modularity Modularity is achieved through a system of abstract classes, one for each tier. These provide the structure with which modules accept input data and return derived parameters to be stored in the DB. At Tier 0, the input is the raw alert content, at Tier 2, a transient state, and at Tier 3, a transient view. The expected output follows a similar pattern: At Tier 0 a boolean value determining whether a transient is accepted and at Tier 2 a science record (dictionary), which is linked in the DB to the state from which it was derived. As T3, output is not state-bound, but rather is added to the transient *journal*, a time-ordered history accompanying each transient. These can make direct use of currently well developed libraries such as `numpy` (Oliphant 2006–), `scipy` (Jones et al. 2001–), and `astropy` (Astropy Collaboration et al. 2013; Price-Whelan et al. 2018). Developers can choose to make their contributed software available to other users, and gain recognition for functional code, or keep them private. The modularity means that users can independently vary the source of alerts, calibration version, selection criteria and analysis software, and can also compare the output to exactly trace the impact of each.

Schemas and AMPEL shapers Contributed modules will be limited as long as they have to be tuned for a specific kind of input, e.g., ZTF photometry. Eventually, we hope that more general code can be written through the development of richer schemas for astronomical information based on which modules can be developed and immediately applied to different source streams. The International Virtual Observatory Alliance (IVOA) initiated the development of the `VOEvent` standard with this purpose[6]. Core information of each event is to be mapped to a set of specific tags (such as *Who*,*What*, *Where*, *When*) ,stored in an `XML` document. `VOEvents` form a starting point for this development, but more work is needed before a general T2 module can be expected to

[6] http://www.ivoa.net/documents/VOEvent/20110711/REC-VOEvent-2.0.pdf

immediately work on data from all sources. As an intermediate solution, AMPEL employes *shapers* that can translate source-specific parameters to a generalised data format that all modules can rely on. While the internal AMPEL structure is designed for performance and flexibility, it is easy to construct T3 modules that export transient information according to, for example, VOEvent or GCN specifications.

The archive Full replayability requires that all alerts are available at later times. While most surveys are expected to provide this, we keep local copies of all alerts until other forms of access are guaranteed.

Catalogs, Watch-lists and ToO triggers Understanding astronomical transients frequently requires matches to known source catalogs. AMPEL currently provides two resources to this end. A set of large, pre-packaged catalogs can be accessed using catsHTM, including the Gaia DR2 release (Soumagnac & Ofek 2018). As a complement, users can upload their own catalogs using extcats[7] for use either transient filtering or to annotate transients with additional information. extcats is also used to create *watch-lists* and *ToO channels*. Watchlists are implemented as a T0 filter that matches the transient stream with a contributed extcat catalog. A ToO channel has a similar functionality, but employs a dynamic extcat target list where a ToO trigger immediately adds one or more entries to the matchlist. The stream can in this case initially be replayed from some previous time (a *delayed T0*), which allows preexisting transients to be consistently detected.

The live database The live transient DB is built using the NoSQL MongoDB[8] engine. The flexibility of not having an enforced schema allows AMPEL to integrate varying alert content and give full freedom to algorithms to provide output of any shape. The live AMPEL instance is a closed system that users cannot directly interact with, and contributed modules do not directly interact with the DB. Instead, the AMPEL core system manages interactions through the alert, state and transient view objects introduced above. [9] Each channel also specifies conditions for when a transient is no longer considered "live". At this point it is *purged*: extracted from the live DB together with all states, computations and logs, and then inserted into a channel specific offline DB which is provided to the channel owner.

AMPEL instances and containers An AMPEL instance is created through combining tagged versions of core and contributed modules into a Docker (Merkel 2014) image, which is then converted to Singularity (Kurtzer et al. 2017) format for execution by an unprivileged user. The final product is a unique "container" that is immutable and encapsulates the AMPEL software and its dependencies. These can be reused and referenced for later work, even if the host environment changes significantly. The containers are coordinated with a simple orchestration tool[10] that exposes an interface similar to Docker's "swarm mode." Previously-deployed AMPEL versions are stored, and can be run off-line on any sequence of archived or simulated alerts. Several instances of AMPEL might be active simultaneously, with each processing either a fraction of a full live-stream, or some set of archived or simulated alerts. Each works with a distinct database. The current ZTF alert flow can easily be parsed by a single instance, called *the live instance*. A full AMPEL analysis combines this active parsing and reacting to the live streams with subsequent or parallel runs in which the effects of the channel parameters can be systematically explored.

Logs and provenance AMPEL contains extensive, built-in *logging* functions. All AMPEL modules are provided a logger, and we recommend this to be consistently used. Log entries are automatically tagged with the appropriate channel and transient ID, and are then inserted into the DB. These tools, together with the DB content, alert archive and AMPEL container, makes provenance straightforward. The IVOA has initiated the development of a Provenance Data Model (DM) for astronomy, following the definitions proposed by the W3C (Sanguillon et al. 2017)[11]. Scientific information is here described as flowing between *agents*, *entities* and *activities*. These are related through causal relations. The AMPEL internal components can be directly mapped to the categories of the IVOA Provenance DM: Transients, datapoints, states and ScienceRecords are entities, Tier modules are activities and users, AMPEL maintainers, software developers and alert stream producers are agents. A streaming analysis carried out in AMPEL will always fulfill these provenance requirements.

Hardware requirements The current live instance installed at the DESY computer center in Zeuthen consists of two machines, "Burst" and "Transit". Real time alert processing is done at Burst (32 cores, 96 GB memory, 1TB SSD) while alert reception and archiving is done at Transit (20 cores, 48GB memory, 1TB SSD + medium-time storage). This system has been designed for extragalactic programs based on the ZTF survey, with a few $\times 10^5$ alerts processed each night, of which between 0.1 and 1% are accepted. Reprocessing large alert volumes from the archive on Transit is done at a mean rate of 100 alerts per second. As the ZTF live alert production rate is lower than this, and Burst is a more powerful machine, this setup is never running at full capacity. It would be straightforward to distribute processing of T2 and T3 tasks among multiple machines, but as the expected practical limitation is access to a common database, this is of limited use until extremely demanding modules are requested.

[7] https://github.com/MatteoGiomi/extcats
[8] https://docs.mongodb.com/manual/
[9] Eventually, daily snapshot copies of the DB will be made available for users to interactively examine the latest transient information without being limited with what was reconfigured to be exported.
[10] https://github.com/AmpelProject/singularity-stack
[11] http://www.ivoa.net/documents/ProvenanceDM/20181015/PR-ProvenanceDM-1.0-20181015.pdf

5. Using AMPEL

5.1. Creating a channel for the ZTF alert stream

A set of sample channel configurations and modules are available in the Ampel-contrib-sample repository.[12]. The process for implementing a channel can be summarized through the following steps:

1. Fork the sample repository and rename it *Ampel-contrib-groupID* where *groupID* is a string identifying the contributing science team.
2. Add modules to the t0/t2/t3 sub-directories, with each module inheriting from the provided base and example classes.
3. Construct the repository channels by defining their parameters in two configuration files: channels.json which regulates the T0, T1 and T2 tiers, and t3_jobs.json which determines the schedule for T3 tasks. These can be constructed to make use of AMPEL modules present either in this repository, or from other public AMPEL contrib repositories.
4. Notify AMPEL administrators. The last step will trigger channel testing and potential edits. After the channel is verified, it will be added in the list of AMPEL contribution modules and included in the next image build. The same channel can also (or exclusively) be applied to archived ZTF alerts.

5.2. Using AMPEL for other streams

Nothing in the core AMPEL design is directly tied to the ZTF stream, or even optical data. The only source-specific software classes is the Kafka client reading the alert stream, and the alert shapers which make sure key variables such as coordinates are stored in a uniform matter. Using a non-structured DB means that any stream content will be stored by AMPEL, and can be used for further processing. A more complex question concerns how to design modules that can be directly applied to different stream sources. As an example, different optical surveys might use different conventions for how to encode which filter was used, and the reference system and uncertainty of reported magnitudes and powerful alert metrics, such as the RealBogus value of ZTF, are unique. Until common standards are developed modules will have to be modified or expanded directly to every new alert stream.

6. Initial AMPEL applications

6.1. Exploring the ZTF alert parameter space

It has been notoriously challenging to quantify transient detection efficiencies, search old surveys for new kinds of transients, and predict the likely yield from a planned follow-up campaign. We here demonstrate how AMPEL can assist with such tasks. For this case study we process 4 months of public ZTF alerts using a set of AMPEL filters spanning the parameter space of the main properties of ZTF alerts. The accepted samples of each channel are, in a second step, compared with confirmed Type Ia supernovae (SNIa) reported to the TNS during the same period. We can thus examine how different channel permuations differ in detection efficiency, and at what phase each SNIa was "discovered". The base comparison sample consists of 134 SNe Ia. The creation of this sample is described in detail in Appendix A.

We processed the ZTF alert archive from June 2nd 2018 (survey start) to Oct 1 using 90 realistic filter versions based on the DecentFilter class. In total 28667252 alerts were included. Each channel exists on a grid constructed by varying the properties described in Table 1. We also include 24 *OR* combinations where the accept critera of two filters are combined. We further consider two additional versions of each filter or filter-combination:

1. Transients in galaxies with known active nuclei (SDSS or MILLIQUAS) are rejected, and
2. Ttransient are required to be associated with a galaxy for which there is a known NED or SDSS spectroscopic redshift $z < 0.1$.

In total, this amounts to 342 combinations. Reprocessing the alert stream in this way took X, demonstrating that AMPEL can already process data at the expected LSST alert rate with current deployment architecture and hardware . All of these variants include some version of alert rejection based on coincidence with a star like object in either Gaia or PanSTARRS. We also tested channels not including any such rejection, which lead to transient counts around 10^5 (an order of magnitude greater than with the star-rejection veto).

This study is neither complete nor unbiased: A large fraction of the SNe were classified by ZTF, and we know that the real number of SNe Ia detected is much larger than the classified subset. Nonetheless it serves both as a benchmark test for channel creation, as well as a starting point for more thorough analysis. An estimate of the total number of supernovae we expect to be hidden in the ZTF detections can be obtained through the simsurvey code, in which known transient rates are combined with a realistic survey cadence and a set of detection thresholds.[13]. The predicted number of Type Ia supernovae fulfilling the criteria of one or more of these channels over the same timespan as the comparison sample and with weather conditions matching the observed was found to be 1033 (average over 10 simulations). Even though they did not form not part of the comparison sample, the simulation also returns estimates for other supernova types. Under the same conditions, we estimate 276 Type Ibc, 92 Type IIn and 377 Type IIP supernovae (average over 10 simulations). The total number of supernovae present in the alert sample is thus estimated to be 1778.

The results for channel efficiencies, compared to the total number of accreted transients, can be found in figure 2. Though we observe the obvious trend that channels with larger coverage of the comparison sample also accept a larger total number of

[12] https://github.com/AmpelProject/Ampel-contrib-sample
[13] https://github.com/ufeindt/simsurvey

Table 1. Dominant channel selection variables and potential settings.

Channel property	Options
RealBogus	*Nominal:* Require ML score above 0.3 or *Strong:* above 0.5
Detections	More than [2, 4, 6, 8] (any filter)
Alert History	*New:* Not older than 5 `days`, *Multi-night:* 4 to 15 `days`, *Persistent:* Older than 8 `days`
Image Quality	*All:* No requirements, *Good:* Limited cuts on e.g. FWHM and bad pixels, *Excellent:* Strong cuts on e.g. FWHM and bad pixels.
Gaia DR2	*Nominal:* Reject likely stars from Gaia DR2, *moderate:* only search in small aperture or *Disabled*.
Star-Galaxy separation	Using PS1 star-galaxy separation (Miller & Tachibana 2019) to reject potential stars (*hard*), likely stars (*nominal*) or no rejection (*disabled*).
Match confusion	*Nominal:* Allow candidates close to nearby (confused) sources, or *disabled*: reject anything close to stars even if other sources exist.

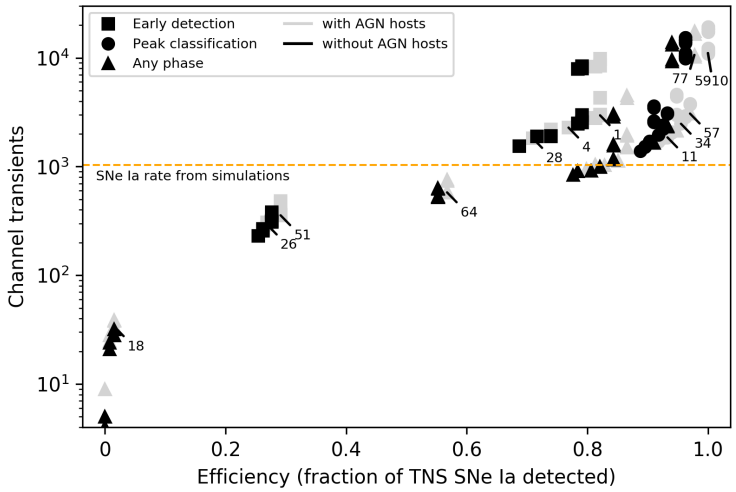

Fig. 2. A comparison of the total number of accepted candidates (y-axis) with fraction of the comparison sample SNe Ia detected as x-axis. Black points indicate channels where transients close to known AGNs where cut, gray that these were accepted. Symbol shape indicate the typical phase at which objects in the comparison sample were detected: Channels where more than 25% were detected prior to phase −10 are marked as early (squares). If instead more than 95% were detected prior to peak light the channel is defined as suitable for peak classification (circles). Channels not fulfilling neither criteria are marked with triangles.

transients, there is also a clear variation in the total transient counts between configurations that find the same fraction of the comparison sample. This figure idenitifies a set of channels with varying completeness levels. Selection statistics for these channels can be found in table 2. The horizontal line in figure 2 indicates the expected total number of SNe Ia as described above. For comparison objects with a well defined time of peak light, we also monitor the phase at which it was accepted into each channel. This information can be used for example to study how well channels perform in finding early SNe Ia, which consitute a prime target for many supernova science studies. In figure 2 we therefore mark all channels where more than 25% of all SNe Ia were discovered prior to phase −10 ("Early detection"). Alternatively, SNIa cosmology programs often look for a combination of completeness and discovery around lightcurve peak to facilitate spectroscopic classification. Channels not fulfilling the Early detection criteria but where more than 95% of all SNe Ia were discovered prior to peak light are therefore marked as "Peak classification". These two simple examples highlight how alert reruns can be used to optimize transient programs, and to estimate yields useful for e.g follow-up proposals. We also find that a significant fraction of the comparison sample (5 out of 134) were found in galaxies with documented AGNs, suggesting that programs which priorise supernova completeness cannot simply reject nuclear transients with active hosts.

Figure 3 and table 3 show channels where only transients in confirmed nearby galaxies are accepted. While total transient and matched SNIa counts are much reduced here, all remaining transient candidates can be said with high probability to be both extragalactic and nearby, and thus good candidates for follow-up. Channels such as "16" and "28" can here be expected to automatically detect multiple early SNIa each year and still have small total counts (160 and 117 transients accepted, respectively).

Table 2. AMPEL sample channel parameter settings and rerun statistics. Columns 2 to 6 show settings used for parameters in Table 1, columns 7 to 10 statistics including all targets and columns 11 to 14 repeating these when excluding AGN associated candidates. The phase estimates describe the fraction of the matched SNIa with a good peak phase estimate that were accepted by the channel either prior to lightcurve peak or to −10 days w.r.t. peak.

Channel	RealBogus	Detections	History	Image	Gaia	SNe Ia (all)	Detections (all)	Phase(< 0) (all)	Phase(< −10) (all)	SNe Ia (no AGN)	Detections (no AGN)	Phase(< 0) (no AGN)	Phase(< −10) (no AGN)
11	0.5	4	multinight	good	nominal	125	1857	0.956	0.067	120	1514	0.953	0.047
26	0.3	4	new	excellent	nominal	36	293	1.000	0.296	35	257	1.000	0.308
34	0.5	2	multinight	excellent	nominal	128	2479	0.944	0.079	123	1964	0.941	0.059
18	0.5	6	new	crap	nominal	2	34	0.000	0.000	2	28	0.000	0.000
77	0.3	4	persistent	crap	moderate	131	10672	0.832	0.000	126	9705	0.824	0.000
51	0.3	4	new	good	nominal	39	357	1.000	0.321	37	311	1.000	0.308
57	0.3	4	persistent	good	nominal	130	3078	0.830	0.000	125	2351	0.822	0.000
64	0.3	8	multinight	good	nominal	76	580	0.554	0.000	74	524	0.556	0.000
1	0.3	2	new	good	nominal	110	2968	0.987	0.557	106	2562	0.987	0.533
28	0.5	2	new	excellent	nominal	95	1833	0.985	0.485	92	1547	0.985	0.462
4	0.5	2	new	good	nominal	103	2286	0.986	0.514	99	1909	0.985	0.485
10	0.5	2	multinight	good	nominal								
59	0.3	4	persistent	good	moderate								
10+59						134	11112	0.926	0.084	129	9973	0.923	0.055

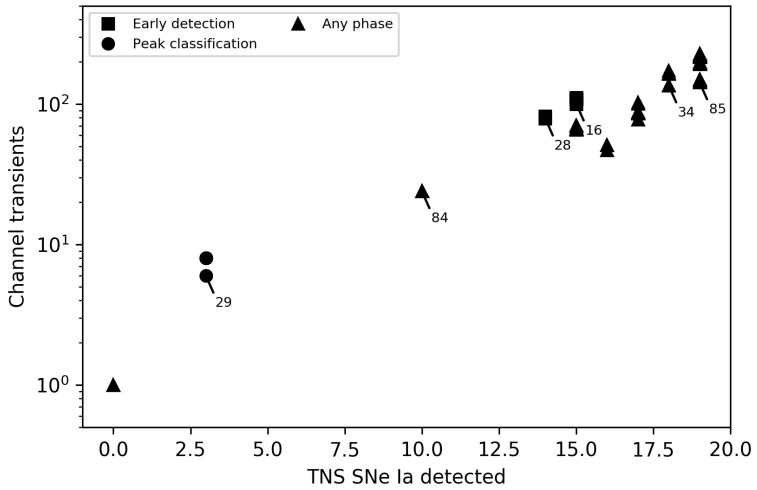

Fig. 3. Comparison of the total number of accepted candidates (y-axis) with the number of comparison sample SNe Ia found, where only candidates linked to a galaxy with known spectroscopic redshift $z < 0.1$. Symbol shape indicates the typical phase at which objects in the comparison sample were detected: Channels where more than 25% where detected prior to phase −10 are marked as early (squares). If this is not true but more than 95% detected prior to peak light the channel is defined as suitable for peak classification (circles). Channels not fulfilling neither criteria are marked with triangles.

Table 3. AMPEL sample channel parameter settings and rerun statistics for cases when only transients close to $z < 0.1$ host galaxies are included. Columns 2 to 6 show settings used for parameters in Table 1, columns 7 to 10 statistics including all targets and columns 11 to 14 repeating these when excluding AGN associated candidates. The phase estimates describe the fraction of the matched SNIa with a good peak phase estimate that were accepted by the channel either prior to lightcurve peak or to −10 days w.r.t. peak.

Channel	RealBogus	Detections	History	Image	Gaia	SNe Ia (all)	Detections (all)	Phase(< 0) (all)	Phase(< −10) (all)	SNe Ia (no AGN)	Detections (no AGN)	Phase(< 0) (no AGN)	Phase(< −10) (no AGN)
85	0.3	4	persistent	good	nominal	21	261	0.750	0.000	19	143	0.714	0.000
34	0.5	2	multinight	excellent	nominal	20	231	0.867	0.067	18	136	0.846	0.077
16	0.5	2	new	crap	nominal	17	160	0.923	0.385	15	101	0.909	0.273
29	0.5	4	new	excellent	nominal	4	9	1.000	0.000	3	6	1.000	0.000
84	0.3	8	multinight	crap	moderate	11	32	0.333	0.000	10	24	0.375	0.000
28	0.5	2	new	excellent	nominal	15	117	0.917	0.333	14	79	0.909	0.273

6.2. Real-time matching with IceCube neutrino detections

The capabilities and flexibility of AMPEL can also be highlighted with the example of the realtime neutrino multi-messenger program. Several years ago, the IceCube Neutrino Observatory discovered a diffuse flux of high-energy astrophysical neutrinos(IceCube Collaboration 2013). Despite recent evidence identifying a flaring blazar as the first neutrino source (IceCube Collaboration et al. 2018), the origin of the bulk of the observed diffuse neutrino flux remains, as yet, undiscovered. One promising approach to identify these neutrino sources is through multi-messenger programs which explore the possibility of detecting multi-wavelength counterparts to detected neutrinos. Likely high-energy neutrino source classes with optical counterpart are typically variables or transients emitting on timescales of hours to months, for example Core Collapse Supernovae, Active Galactic Nuclei or Tidal Disruption Events (Waxman 1995; Janka et al. 2007; Atoyan & Dermer 2001, 2003; Dai & Fang 2017). To detect counterparts on these timescales,

telescopes are required which feature a high cadence and a large field-of-view, in order to cover a significant fraction of the sky. In addition to an optimised volumetric survey speed capable of discovering large numbers of objects, neutrino correlation studies require robustly-classified samples of optical transient populations. In order to provide a prompt response to selected events within large data volumes, a software framework is required that can analyze and combine optical data streams with real-time multi-messenger data streams. In particular, a real-time stream of several hundred neutrinos per day is sent from IceCube to AMPEL, with directional, temporal and energy information (Aartsen et al. 2017).

We have implemented two complementary strategies to optimize the search for, and classification of, optical transients in vicinity of the neutrino positions. Firstly, we employ a target-of-opportunity T0 filter to select ZTF alerts which pass image quality cuts, and are also spatially and temporally coincident with that IceCube High-Energy neutrino alerts distributed via GCN notifications. This enables rapid follow-up of potential interesting counterparts, but is only feasible for the handful of neutrinos which have sufficiently large energy to identify them as having a likely astrophysical origin. A second program seeks to exploit the much more numerous collection of lower-energy astrophysical neutrinos detected by IceCube, which are hidden beneath a much larger sample of atmospheric background neutrinos. To identify these hidden astrophysical neutrinos, we employ a realtime maximum likelihood calculation within the T2 framework of AMPEL. For each ZTF alert which passes the neutrino T0 filter, we search for individual neutrinos or neutrino clusters which are likely to have an astrophysical origin based on their energy, as well as spatial and temporal coincidence with the given transient and its associated lightcurve. In particular, the consistency of the lightcurve with a given transient class, and the consistency of the neutrino arrival times with the emission models expected for that class, enable us to greatly reduce the number of chance coincidences between neutrinos and optical transients. This program allows us to optimize the filtering of ZTF alerts in realtime which are subsequently follow-up spectroscopically, providing us with a magnitude-limited complete, typed catalogue of all optical transients which are coincident with neutrinos.

7. Discussion

7.1. AMPEL TNS submissions

AMPEL submits transient candidates to the TNS which are identified as likely to be new (no detection more than 5 days ago) and of extragalactic origin. The candidates are submitted in approximately real-time under the sender ZTF_AMPEL_MSIP. The selection process is automatic, and uses the parameters of channel "1" as described above. Candidates compatible with known AGN/QSOs are marked as such in the TNS comment field. There is a current magnitude limit (January 2019) at 19.5 for submission, for which the contamination of stellar objects is lower than 5%. The magnitude depth will be increased once a sufficiently-low stellar contamination rate has been confirmed for fainter transients. Extrapolating rates from the four month ZTF rerun, we expect to submit $\sim$ 9000 astronomical transients to the TNS each year.

8. Conclusions

AMPEL is a framework designed for flexible transient brokering, analysis and reaction. Users contribute channels, which then configure transients to be processed at four internal tiers. The implementation was guided by four challenges for transient analysis, which were introduced in Section 2. *Provenance and reproducibility* are guaranteed by the combination of information stored in a permanent database, containerized software and alert archive in a system designed to allow autonomous analysis chains. A modular system provides *analysis flexibility*, and introduces a method for developers to allow software distribution and referencing. The combinations of these two capabilities allows users to track the impact of *versions* of both data and software. Finally, the database has been designed to manage the *alert rates* expected from surveys such as LSST.

An AMPEL user defines a channel consisting at a minimum of an alert filter configuration ("Tier 0") and a "Tier 3" module which exports selected transients to the user. This replicates the behavior of a basic broker. The channel can be made more advanced through updated data values ("Tier 1") and science calculations ("Tier 2"). The flexible structure of AMPEL is made possible through the introduction of a set of information carriers. A transient is connected to a series of *states*, each of which consists of a specified set of *datapoints*. New states are most often created by new observations, but can also be created through removed (rejected) datapoints or datapoints with updated (improved) values. A *transient view* collects the information of a transient available at a given time, combining its states with any other data that was collected such as T2 module results. Creating an AMPEL channel carries an initial cost where users have to be proactive. However, this cost is offset by the numerous advantages afforded by a custom channel: it is applied to the full ZTF alert stream, the container formalism makes sure it can be run at later times and it is ensured to fulfill modern provenance standards.

Two sample uses of AMPEL were introduced. We first showed how a reprocessing of alerts from the first four months of ZTF operations can be used to create a "cooking book" of filter definitions with defined acceptance and completeness rates. As part of this study, we show that ZTF discovered and issued alerts for all SNe Ia reported to the TNS, and that AMPEL can operate at the high data rates expected for LSST. As a second example, we introduce the live correlation analysis between optical ZTF candidates and candidate extragalactic neutrinos from IceCube, where a T2 module calculates test statistics between all potential matches.

AMPEL has now started relaying good extragalactic transient candidates to the TNS, where they are available for the community. The chosen channel configuration was shown to detect $\sim$ 80% the SNe in the comparison sample, with more than 25% detected prior to phase -10 days. We expect this to provide $\sim$ 9000 astronomical transients to the TNS during a full year of operations.

Acknowledgements. Based on observations obtained with the Samuel Oschin Telescope 48-inch and the 60-inch Telescope at the Palomar Observatory as part of the Zwicky Transient Facility project. ZTF is supported by the National Science Foundation under Grant No. AST-1440341 and a collaboration including Caltech, IPAC, the Weizmann Institute for Science, the Oskar Klein Center at Stockholm University, the University of Maryland, the University of Washington, Deutsches Elektronen-Synchrotron and Humboldt University, Los Alamos National Laboratories, the TANGO Consortium of Taiwan, the University of Wisconsin

at Milwaukee, and Lawrence Berkeley National Laboratories. Operations are conducted by COO, IPAC, and UW. N. M. acknowledges the support of the Helmholtz Einstein International Berlin Research School in Data Science (HEIBRiDS), Deutsches Elektronensynchrotron (DESY), and Humboldt-Universität zu Berlin.

References

Aartsen, M. G., Ackermann, M., Adams, J., et al. 2017, Astroparticle Physics, 92, 30
Abbott, B. P., Abbott, R., Abbott, T. D., et al. 2017, ApJ, 848, L12
Allen, G., Anderson, W., Blaufuss, E., et al. 2018, arXiv e-prints, arXiv:1807.04780
Astropy Collaboration, Robitaille, T. P., Tollerud, E. J., et al. 2013, A&A, 558, A33
Atoyan, A. & Dermer, C. D. 2001, Phys. Rev. Lett., 87, 221102
Atoyan, A. M. & Dermer, C. D. 2003, ApJ, 586, 79
Bellm, E. C., Kulkarni, S. R., Graham, M. J., et al. 2019, PASP, 131, 018002
Dai, L. & Fang, K. 2017, MNRAS, 469, 1354
IceCube Collaboration. 2013, Science, 342, 1242856
IceCube Collaboration, Aartsen, M. G., Ackermann, M., et al. 2018, Science, 361, eaat1378
Janka, H. T., Langanke, K., Marek, A., Martínez- Pinedo, G., & Müller, B. 2007, Phys. Rep., 442, 38
Jones, E., Oliphant, T., Peterson, P., et al. 2001–, SciPy: Open source scientific tools for Python, [Online; accessed 2019-01-22>]
Jurić, M., Kantor, J., Lim, K. T., et al. 2017, in Astronomical Society of the Pacific Conference Series, Vol. 512, Astronomical Data Analysis Software and Systems XXV, ed. N. P. F. Lorente, K. Shortridge, & R. Wayth, 279
Kurtzer, G. M., Sochat, V., & Bauer, M. W. 2017, PLOS ONE, 12, 1
Masci, F. J., Laher, R. R., Rusholme, B., et al. 2019, PASP, 131, 018003
Merkel, D. 2014, Linux J., 2014
Miller, A. & Tachibana, Y. 2019, in American Astronomical Society Meeting Abstracts, Vol. 233, American Astronomical Society Meeting Abstracts #233, 457.01
Oliphant, T. 2006–, NumPy: A guide to NumPy, USA: Trelgol Publishing, [Online; accessed 2019-01-22]
Patterson, M. T., Bellm, E. C., Rusholme, B., et al. 2019, PASP, 131, 018001
Price-Whelan, A. M., Sipőcz, B. M., Günther, H. M., et al. 2018, AJ, 156, 123
Saha, A., Matheson, T., Snodgrass, R., et al. 2014, in Society of Photo-Optical Instrumentation Engineers (SPIE) Conference Series, Vol. 9149, Observatory Operations: Strategies, Processes, and Systems V, 914908
Sanguillon, M., Servillat, M., Louys, M., et al. 2017, in Astronomical Society of the Pacific Conference Series, Vol. 512, Astronomical Data Analysis Software and Systems XXV, ed. N. P. F. Lorente, K. Shortridge, & R. Wayth, 581
Smith, M. W. E., Fox, D. B., Cowen, D. F., et al. 2013, Astroparticle Physics, 45, 56
Soumagnac, M. T. & Ofek, E. O. 2018, Publications of the Astronomical Society of the Pacific, 130, 075002
Waxman, E. 1995, Phys. Rev. Lett., 75, 386

Appendix A: Creating the TNS comparison sample

The comparison sample that is used to estimate channel efficiences was constructed through retrieving all TNS SNe classified as Type Ia supernovae (not including peculiar subtypes) and with a detection date between June 5th and Sep 15h 2018. This was further restricted to SNe above an absolute galactic latitude of 14 degrees. This leaves 310 objects shown in Table A.1. Out of these 20 has positions outside the ZTF MSIP field grid and 8 were projected to land in gaps between ZTF CCDs or within the 1 % of chip pixels closes to a readout edge.

As ZTF field references have been continuously produced during the first season of operations we also verify that subtractions were made at least 3 days prior to the SN detection. For 89 SNe no references were available while for 58 SNe a reference was only available in either *g* or *R* band. One TNS object included in this list, SN2018ekt, was as part of this study found to have been erroneously classified (this has thus now been removed). Excluding this leaves a main comparison sample of 134 SNe Ia that were observed by ZTF in the nominal ZTF MSIP cadence. Among SNe only found in one band SN2018fvh is located on bad pixels, SN2018cmu is only detected in a single alert (one detection) and SN2018cmk was detected by ZTF but more than 3 arcsec from the reported TNS position.

Table A.1. TNS SNe Ia detected between June 5th and Sep 15th.

Name	RA	DEC	Redshift	ZTF field match	Detectable
SN 2018guh	21:53:36.95	+07:14:06.30	0.120	In MSIP grid	Detectable g or R
SN 2018guc	02:30:57.89	+13:26:22.02	0.091	In MSIP grid	Detectable g or R
SN 2018gtg	01:57:26.22	+08:55:02.54	0.108	In MSIP grid	Detectable g+R
SN 2018gsb	16:46:08.75	+19:27:17.22	0.060	In MSIP grid	Detectable g+R
SN 2018gqo	08:27:18.13	+10:59:57.28	0.087	In MSIP grid	Detectable g or R
SN 2018gqn	08:42:44.87	+10:41:42.56	0.060	In MSIP grid	Detectable g or R
SN 2018gqa	17:51:11.31	+53:18:52.09	0.105	In MSIP grid	Detectable g+R
SN 2018gkz	07:58:11.54	+19:31:07.92	0.240	In MSIP grid	Detectable g or R
SN 2018gkw	07:57:37.92	+44:44:48.60	0.072	In MSIP grid	Detectable g or R
SN 2018gkj	22:02:27.07	-64:21:06.77	0.042	In MSIP grid	No reference
SN 2018gka	02:59:20.01	-14:05:59.27	0.100	In MSIP grid	No reference
SN 2018gjz	20:51:09.99	-24:53:38.86	0.083	Chip / RC border	Not clear
SN 2018git	01:40:04.26	+15:04:16.67	0.071	In MSIP grid	Detectable g+R
SN 2018gif	03:27:15.75	+08:42:39.13	0.039	In MSIP grid	No reference
SN 2018ghr	22:59:12.79	+00:24:17.96	0.072	In MSIP grid	Detectable g or R
SN 2018ghp	00:13:42.06	+27:34:03.45	0.069	In MSIP grid	Detectable g or R
SN 2018ghh	10:14:20.24	+56:19:16.44	0.050	In MSIP grid	Detectable g+R
SN 2018ggz	01:47:53.66	+42:11:45.49	0.074	In MSIP grid	Detectable g or R
SN 2018ggx	01:04:38.80	-04:15:29.42	0.038	In MSIP grid	Detectable g or R
SN 2018ggw	18:28:15.30	+46:21:12.27	0.053	In MSIP grid	Detectable g+R
SN 2018ggt	00:57:02.61	-00:52:25.68	0.044	In MSIP grid	Detectable g+R
SN 2018ggq	18:37:17.16	+49:08:54.31	0.090	In MSIP grid	Detectable g+R
SN 2018ggc	08:38:10.69	+24:53:26.72	0.030	In MSIP grid	Detectable g or R
SN 2018gfw	20:30:53.58	-26:31:04.42	0.032	In MSIP grid	No reference
SN 2018gfs	15:52:03.30	+30:44:05.71	0.080	In MSIP grid	Detectable g+R
SN 2018gfi	00:58:53.95	-24:11:47.22	0.020	Outside MSIP grid	Not observable
SN 2018gfg	20:59:09.74	-14:15:47.47	0.082	In MSIP grid	Detectable g or R
SN 2018gff	02:05:40.56	+19:05:31.82	0.069	In MSIP grid	Detectable g or R
SN 2018gfe	16:17:48.37	+41:28:10.37	0.065	In MSIP grid	Detectable g+R
SN 2018ges	21:33:50.41	+24:20:03.41	0.115	Chip / RC border	Not clear
SN 2018geo	16:18:13.84	+39:07:25.74	0.031	In MSIP grid	Detectable g+R
SN 2018gec	07:09:53.50	+54:58:07.46	0.037	Outside MSIP grid	Not observable
SN 2018gdg	00:30:24.63	-01:15:50.88	0.057	In MSIP grid	Detectable g+R
SN 2018gck	00:50:56.61	+03:29:55.02	0.100	In MSIP grid	Detectable g or R
SN 2018gcg	17:16:10.37	+01:25:46.25	0.094	In MSIP grid	Detectable g+R
SN 2018fzw	05:42:48.04	-24:29:34.39	0.046	In MSIP grid	No reference
SN 2018fzm	21:03:19.79	-51:32:48.23	0.047	In MSIP grid	No reference
SN 2018fzi	23:39:47.31	-23:55:12.81	0.080	In MSIP grid	Detectable g or R
SN 2018fyg	02:45:59.36	+42:32:29.67	0.039	In MSIP grid	No reference
SN 2018fwn	03:29:34.39	-19:41:41.35	0.044	In MSIP grid	No reference
SN 2018fwi	22:47:46.56	-31:15:33.70	0.115	In MSIP grid	No reference
SN 2018fvy	01:32:16.23	-33:06:05.61	0.036	In MSIP grid	No reference
SN 2018fvw	21:02:20.23	+19:57:46.25	0.040	In MSIP grid	Detectable g+R
SN 2018fvr	15:52:22.18	+22:55:56.41	0.053	In MSIP grid	Detectable g+R
SN 2018fvq	21:31:32.38	-27:15:43.56	0.073	In MSIP grid	No reference
SN 2018fvm	20:37:27.79	-37:43:16.93	0.018	In MSIP grid	No reference
SN 2018fvl	21:01:12.26	+14:29:07.68	0.066	In MSIP grid	Detectable g+R
SN 2018fvj	04:29:31.07	-11:01:50.56	0.066	In MSIP grid	No reference
SN 2018fvi	01:57:42.56	-67:11:12.80	0.040	In MSIP grid	No reference
SN 2018fvh	01:15:10.21	-18:10:59.56	0.073	In MSIP grid	Detectable g or R
SN 2018fvb	16:00:00.65	-11:05:27.71	0.051	In MSIP grid	No reference
SN 2018fva	23:32:34.75	+08:45:10.38	0.074	In MSIP grid	No reference
SN 2018fuu	23:24:56.60	+09:25:52.68	0.060	In MSIP grid	Detectable g or R
SN 2018fum	01:36:11.29	+27:16:29.51	0.060	In MSIP grid	Detectable g or R
SN 2018fuk	05:45:08.16	-79:23:47.52	0.018	In MSIP grid	No reference
SN 2018fuj	04:30:58.48	-26:46:54.10	0.051	Outside MSIP grid	Not observable

Name	RA	DEC	Redshift	ZTF field match	Detectable
SN 2018fub	00:40:30.65	-50:41:15.14	0.029	In MSIP grid	No reference
SN 2018fty	02:26:47.30	-09:04:02.32	0.054	In MSIP grid	Detectable g or R
SN 2018ftu	01:34:41.55	-05:38:05.25	0.063	In MSIP grid	Detectable g or R
SN 2018ftt	17:36:27.05	+22:29:25.96	0.056	In MSIP grid	Detectable g+R
SN 2018fte	01:44:08.27	+07:58:37.46	0.062	In MSIP grid	Detectable g or R
SN 2018ftd	02:01:16.11	-01:13:26.26	0.062	In MSIP grid	Detectable g or R
SN 2018ftc	23:28:03.88	+09:46:13.30	0.050	Outside MSIP grid	Not observable
SN 2018fst	01:19:32.29	-18:10:24.46	0.100	In MSIP grid	Detectable g or R
SN 2018fss	03:06:26.81	+41:12:49.79	0.060	In MSIP grid	Detectable g or R
SN 2018fsr	07:49:07.34	+32:58:50.22	0.028	In MSIP grid	Detectable g or R
SN 2018fsf	22:40:24.67	+16:11:26.86	0.095	In MSIP grid	Detectable g+R
SN 2018fse	17:14:14.51	+36:27:32.30	0.084	In MSIP grid	Detectable g+R
SN 2018fsa	22:25:37.11	-13:04:28.27	0.043	In MSIP grid	No reference
SN 2018frx	17:23:49.83	+46:18:05.72	0.085	In MSIP grid	Detectable g+R
SN 2018frv	20:40:31.43	-46:34:39.22	0.043	In MSIP grid	No reference
SN 2018frk	22:46:16.77	-07:50:13.91	0.080	Outside MSIP grid	Not observable
SN 2018fqn	22:39:38.02	-15:05:08.66	0.052	Outside MSIP grid	Not observable
SN 2018fql	23:41:16.08	-28:57:44.74	0.049	In MSIP grid	No reference
SN 2018fqk	22:33:09.02	+04:07:47.03	0.041	In MSIP grid	No reference
SN 2018fqj	14:23:49.00	+34:06:10.35	0.100	In MSIP grid	Detectable g+R
SN 2018fqe	15:38:03.03	+51:21:37.30	0.074	In MSIP grid	Detectable g+R
SN 2018fqd	20:51:51.48	-36:50:13.31	0.039	Chip / RC border	Not clear
SN 2018fqc	05:20:45.15	-23:04:04.67	0.085	In MSIP grid	No reference
SN 2018fpv	15:08:04.21	+37:15:05.80	0.079	In MSIP grid	Detectable g+R
SN 2018fpe	15:01:03.65	+44:09:23.54	0.088	In MSIP grid	Detectable g+R
SN 2018fop	01:15:18.11	-06:51:32.54	0.020	In MSIP grid	No reference
SN 2018fod	16:13:41.56	+10:39:30.68	0.080	In MSIP grid	Detectable g or R
SN 2018foc	02:44:07.12	+37:31:27.46	0.031	In MSIP grid	Detectable g or R
SN 2018fnq	20:12:30.00	-44:06:35.14	0.019	Chip / RC border	Not clear
SN 2018fng	16:07:03.01	+15:35:44.68	0.040	In MSIP grid	Detectable g+R
SN 2018fnf	23:40:45.92	+14:06:01.34	0.063	In MSIP grid	Detectable g or R
SN 2018fne	18:31:33.45	+49:48:57.94	0.045	In MSIP grid	Detectable g+R
SN 2018fnd	16:47:54.59	+42:58:07.61	0.075	In MSIP grid	Detectable g+R
SN 2018fnc	18:16:07.46	+70:01:04.60	0.080	In MSIP grid	Detectable g+R
SN 2018fmu	19:45:40.96	+66:30:29.85	0.085	In MSIP grid	No reference
SN 2018fmr	21:54:00.01	+08:06:52.87	0.070	In MSIP grid	Detectable g+R
SN 2018fli	15:58:11.68	+19:45:54.75	0.066	In MSIP grid	Detectable g or R
SN 2018flg	16:14:46.99	+43:18:19.06	0.060	In MSIP grid	Detectable g+R
SN 2018fjx	22:27:36.81	+22:53:43.12	0.057	In MSIP grid	Detectable g or R
SN 2018fjv	16:45:29.83	+65:14:20.60	0.070	In MSIP grid	Detectable g+R
SN 2018fju	16:19:44.23	+50:33:06.72	0.056	In MSIP grid	Detectable g+R
SN 2018fjc	21:38:53.12	+31:44:15.09	0.042	In MSIP grid	Detectable g or R
SN 2018fja	21:59:01.79	+11:06:13.32	0.076	In MSIP grid	Detectable g+R
SN 2018fiw	00:15:01.84	+34:48:40.33	0.048	In MSIP grid	Detectable g+R
SN 2018fiv	21:54:36.51	+18:06:56.78	0.050	In MSIP grid	Detectable g+R
SN 2018fio	15:21:14.35	+30:38:11.91	0.075	In MSIP grid	Detectable g+R
SN 2018fin	16:51:00.83	+25:52:33.51	0.060	In MSIP grid	Detectable g+R
SN 2018fim	16:37:39.98	+25:19:15.26	0.068	In MSIP grid	Detectable g+R
SN 2018fhx	06:24:38.04	-23:43:58.94	0.023	In MSIP grid	No reference
SN 2018fhw	04:18:06.27	-63:36:54.25	0.017	In MSIP grid	No reference
SN 2018fhh	18:48:19.09	+30:36:25.25	0.100	In MSIP grid	Detectable g+R
SN 2018fhg	15:03:45.14	+61:34:04.41	0.066	In MSIP grid	Detectable g+R
SN 2018fhe	19:50:48.25	+64:55:22.29	0.068	In MSIP grid	Detectable g+R
SN 2018fgj	04:47:32.42	-02:18:22.50	0.031	In MSIP grid	No reference
SN 2018ffo	01:05:42.50	+07:32:55.65	0.040	In MSIP grid	No reference
SN 2018ffn	00:24:07.84	-07:52:49.64	0.100	Outside MSIP grid	Not observable
SN 2018ffi	21:40:11.30	+21:33:30.22	0.090	Chip / RC border	Not clear
SN 2018ffb	22:58:11.52	-20:17:02.76	0.070	In MSIP grid	No reference
SN 2018fey	01:22:19.50	-02:29:48.62	0.060	In MSIP grid	No reference
SN 2018few	01:04:15.49	-42:44:28.14	0.066	In MSIP grid	No reference
SN 2018fev	13:46:54.60	+32:26:34.30	0.110	In MSIP grid	Detectable g+R
SN 2018fem	13:01:12.62	+39:45:23.25	0.070	In MSIP grid	Detectable g+R
SN 2018fel	16:52:31.24	+23:23:00.67	0.100	In MSIP grid	Detectable g+R
SN 2018fec	18:00:35.19	+61:41:51.76	0.075	In MSIP grid	Detectable g+R
SN 2018feb	17:10:11.16	+21:38:56.53	0.015	In MSIP grid	Detectable g+R
SN 2018fdz	18:15:18.54	+29:54:38.69	0.065	In MSIP grid	Detectable g+R
SN 2018fdy	00:53:13.01	+20:42:52.95	0.082	In MSIP grid	Detectable g or R
SN 2018fdv	00:14:44.78	+17:52:05.69	0.094	In MSIP grid	Detectable g or R
SN 2018fcw	00:50:55.08	-07:46:00.98	0.050	In MSIP grid	No reference
SN 2018fcu	04:17:54.69	-49:54:28.48	0.050	In MSIP grid	No reference
SN 2018fcd	15:40:11.09	+61:31:48.05	0.085	In MSIP grid	Detectable g+R
SN 2018fbj	22:19:58.95	+40:04:22.60	0.099	In MSIP grid	No reference
SN 2018fbh	15:36:31.98	+41:47:59.63	0.041	In MSIP grid	Detectable g+R
SN 2018fae	17:30:42.75	+62:49:52.07	0.082	In MSIP grid	Detectable g+R
SN 2018ezz	18:37:51.87	+51:50:16.80	0.053	In MSIP grid	Detectable g+R
SN 2018ezy	18:58:52.52	+69:00:48.58	0.079	In MSIP grid	Detectable g+R
SN 2018ezx	04:08:08.09	-08:49:59.45	0.033	In MSIP grid	No reference

Name	RA	DEC	Redshift	ZTF field match	Detectable
SN 2018eyh	14:54:37.03	+69:38:53.83	0.060	In MSIP grid	Detectable g+R
SN 2018exv	23:33:57.44	-26:26:49.28	0.070	In MSIP grid	No reference
SN 2018exh	15:07:39.13	+38:12:48.95	0.100	In MSIP grid	Detectable g+R
SN 2018exc	21:00:08.02	-40:21:30.94	0.057	In MSIP grid	No reference
SN 2018exb	21:13:08.54	-20:42:38.90	0.047	In MSIP grid	No reference
SN 2018evw	21:15:14.40	+02:11:34.44	0.050	In MSIP grid	No reference
SN 2018evt	13:46:39.32	-09:38:36.56	0.029	In MSIP grid	No reference
SN 2018evo	21:48:38.42	-43:22:48.07	0.077	In MSIP grid	No reference
SN 2018evf	23:09:35.81	+05:35:12.16	0.060	In MSIP grid	No reference
SN 2018evd	23:16:51.85	+41:03:33.72	0.060	In MSIP grid	No reference
SN 2018evc	22:54:11.70	+05:03:51.07	0.049	In MSIP grid	No reference
SN 2018evb	22:51:02.72	-03:38:58.15	0.090	In MSIP grid	No reference
SN 2018euz	16:14:33.77	+36:56:36.24	0.038	In MSIP grid	Detectable g+R
SN 2018euj	19:52:29.60	-60:45:51.40	0.034	In MSIP grid	No reference
SN 2018eui	03:13:33.24	-15:15:21.64	0.031	In MSIP grid	No reference
SN 2018etm	16:14:20.68	+03:13:55.08	0.020	In MSIP grid	Detectable g+R
SN 2018etj	14:04:23.17	+60:01:27.66	0.042	In MSIP grid	Detectable g+R
SN 2018esx	01:12:12.47	-30:29:40.07	0.090	In MSIP grid	No reference
SN 2018esq	23:29:38.76	-25:10:25.38	0.130	In MSIP grid	No reference
SN 2018esa	22:41:02.82	+20:43:32.02	0.070	In MSIP grid	Detectable g or R
SN 2018ery	15:51:06.33	+08:58:31.74	0.070	In MSIP grid	Detectable g or R
SN 2018ert	16:35:22.54	+22:28:06.23	0.094	In MSIP grid	Detectable g+R
SN 2018ers	16:09:52.84	+65:56:18.48	0.088	In MSIP grid	Detectable g+R
SN 2018err	15:36:53.10	+66:03:29.11	0.106	In MSIP grid	Detectable g+R
SN 2018ero	20:08:41.22	+03:16:17.60	0.060	Outside MSIP grid	Not observable
SN 2018erl	21:12:09.69	-08:27:42.34	0.029	In MSIP grid	No reference
SN 2018erc	02:07:28.51	+11:09:13.64	0.041	In MSIP grid	No reference
SN 2018erb	02:38:11.44	+26:01:09.12	0.041	In MSIP grid	No reference
SN 2018eqq	03:06:55.16	+41:30:32.90	0.016	In MSIP grid	No reference
SN 2018eqg	15:08:14.57	+34:52:05.20	0.092	In MSIP grid	Detectable g+R
SN 2018epx	23:29:53.22	+27:22:40.90	0.024	In MSIP grid	No reference
SN 2018epw	23:06:30.46	+10:18:18.96	0.063	In MSIP grid	No reference
SN 2018eps	16:20:43.18	+65:38:20.96	0.070	In MSIP grid	Detectable g+R
SN 2018epj	15:04:23.61	+61:37:17.21	0.074	In MSIP grid	Detectable g+R
SN 2018epa	21:51:16.88	-14:27:36.22	0.040	In MSIP grid	No reference
SN 2018eoy	20:39:28.80	-13:07:58.31	0.070	In MSIP grid	No reference
SN 2018eod	20:53:19.67	-33:25:24.86	0.054	Outside MSIP grid	Not observable
SN 2018enk	00:25:51.83	-20:40:50.34	0.050	In MSIP grid	No reference
SN 2018enj	20:05:41.10	-47:58:41.30	0.030	In MSIP grid	No reference
SN 2018eni	18:19:11.78	+54:05:19.29	0.085	In MSIP grid	Detectable g+R
SN 2018enc	15:19:28.63	-09:52:50.03	0.017	Outside MSIP grid	Not observable
SN 2018enb	21:39:34.57	+08:52:47.30	0.023	Chip / RC border	Not clear
SN 2018emy	14:45:30.39	+17:15:29.60	0.040	In MSIP grid	Detectable g+R
SN 2018emx	15:26:58.79	+08:15:41.37	0.088	In MSIP grid	Detectable g+R
SN 2018emv	15:05:30.44	+30:54:36.92	0.057	In MSIP grid	Detectable g+R
SN 2018emo	01:05:38.12	+29:29:50.82	0.067	In MSIP grid	No reference
SN 2018eml	15:46:07.11	+29:44:00.49	0.032	In MSIP grid	Detectable g+R
SN 2018emj	16:00:03.58	+23:22:50.62	0.100	In MSIP grid	Detectable g or R
SN 2018emi	17:06:36.33	+24:32:43.15	0.038	In MSIP grid	Detectable g+R
SN 2018emf	00:31:38.41	+28:58:10.50	0.072	In MSIP grid	No reference
SN 2018elm	22:37:21.10	+22:22:46.45	0.043	In MSIP grid	Detectable g+R
SN 2018ell	16:49:57.03	+27:38:26.94	0.064	In MSIP grid	Detectable g+R
SN 2018elj	22:08:23.37	+11:22:45.43	0.040	In MSIP grid	Detectable g+R
SN 2018elh	21:06:09.64	+70:21:08.71	0.050	In MSIP grid	No reference
SN 2018ekt	16:11:28.40	+45:27:11.70	0.015	In MSIP grid	Detectable g+R
SN 2018efm	13:32:50.51	+07:18:39.27	0.030	In MSIP grid	No reference
SN 2018efk	12:22:36.82	+47:58:09.35	0.050	In MSIP grid	Detectable g+R
SN 2018efe	20:39:39.94	+13:08:08.74	0.050	In MSIP grid	Detectable g+R
SN 2018efb	17:44:44.31	+38:09:50.54	0.100	In MSIP grid	Detectable g+R
SN 2018eew	01:52:03.79	-07:38:33.14	0.060	In MSIP grid	No reference
SN 2018eec	22:39:33.10	-02:45:41.23	0.090	In MSIP grid	No reference
SN 2018edz	16:01:05.44	+11:56:39.17	0.045	In MSIP grid	Detectable g or R
SN 2018edw	19:08:40.56	+78:28:39.78	0.080	In MSIP grid	Detectable g or R
SN 2018edd	14:53:32.29	+03:04:13.94	0.030	In MSIP grid	Detectable g or R
SN 2018ect	22:35:08.40	+17:23:20.66	0.070	In MSIP grid	Detectable g or R
SN 2018ecr	18:23:04.99	+27:28:16.03	0.070	In MSIP grid	Detectable g+R
SN 2018ecq	16:45:42.76	+37:53:25.54	0.100	In MSIP grid	Detectable g+R
SN 2018ecp	15:30:21.23	+27:37:46.26	0.070	In MSIP grid	Detectable g+R
SN 2018ecd	13:19:36.73	-29:07:16.61	0.050	In MSIP grid	No reference
SN 2018ebx	00:55:26.42	-74:18:42.19	0.034	In MSIP grid	No reference
SN 2018ebw	02:41:16.40	+20:30:16.88	0.030	In MSIP grid	No reference
SN 2018ebs	21:39:37.62	+08:56:39.78	0.030	Chip / RC border	Not clear
SN 2018ebo	14:16:48.50	+58:29:07.45	0.080	In MSIP grid	Detectable g+R
SN 2018ebj	03:53:06.79	-45:10:51.28	0.051	In MSIP grid	No reference
SN 2018eaz	18:42:55.21	+50:39:33.60	0.050	In MSIP grid	Detectable g+R
SN 2018eak	16:15:48.49	+19:39:25.85	0.030	In MSIP grid	Detectable g or R
SN 2018eag	18:57:16.32	+46:29:56.75	0.072	In MSIP grid	Detectable g+R

Name	RA	DEC	Redshift	ZTF field match	Detectable
SN 2018ead	18:17:21.46	+54:32:14.89	0.070	In MSIP grid	Detectable g+R
SN 2018dzy	22:00:41.71	+19:39:58.34	0.020	In MSIP grid	Detectable g or R
SN 2018dzr	17:02:22.57	+57:45:05.15	0.070	In MSIP grid	Detectable g+R
SN 2018dzh	14:40:33.36	+13:07:23.14	0.050	Outside MSIP grid	Not observable
SN 2018dyz	15:10:40.48	+08:34:27.76	0.045	In MSIP grid	Detectable g or R
SN 2018dyq	16:31:11.00	+60:35:51.84	0.080	In MSIP grid	Detectable g+R
SN 2018dyp	16:45:10.11	+42:43:04.37	0.060	In MSIP grid	Detectable g+R
SN 2018dym	16:05:04.16	+36:05:38.71	0.090	In MSIP grid	Detectable g+R
SN 2018dyg	14:27:12.79	+16:51:45.61	0.050	In MSIP grid	Detectable g or R
SN 2018dye	14:29:14.17	+46:03:03.09	0.077	In MSIP grid	Detectable g+R
SN 2018dxu	14:30:09.92	+55:53:11.63	0.108	In MSIP grid	Detectable g+R
SN 2018dvf	23:14:05.43	+29:38:00.03	0.046	In MSIP grid	Detectable g+R
SN 2018dvd	13:54:34.55	+42:46:28.73	0.070	In MSIP grid	Detectable g+R
SN 2018dvb	15:33:56.92	+31:10:11.42	0.065	In MSIP grid	Detectable g+R
SN 2018dsw	17:35:14.17	+54:14:48.55	0.090	In MSIP grid	Detectable g+R
SN 2018dsv	17:11:13.49	+38:35:25.95	0.040	Outside MSIP grid	Not observable
SN 2018dje	17:52:50.55	+21:22:57.60	0.040	In MSIP grid	Detectable g+R
SN 2018djd	02:14:33.83	-00:45:56.77	0.026	Outside MSIP grid	Not observable
SN 2018dhw	18:59:57.52	+72:16:02.15	0.029	In MSIP grid	Detectable g+R
SN 2018dgz	15:45:41.62	+11:57:09.73	0.070	In MSIP grid	Detectable g or R
SN 2018dgk	13:52:57.96	+05:17:23.18	0.080	In MSIP grid	Detectable g or R
SN 2018des	17:20:08.95	+09:29:32.25	0.080	In MSIP grid	Detectable g or R
SN 2018der	14:48:05.62	+63:13:00.03	0.052	In MSIP grid	Detectable g+R
SN 2018deq	18:11:57.33	+30:02:43.50	0.067	In MSIP grid	Detectable g+R
SN 2018dem	21:11:58.53	-00:13:05.16	nan	In MSIP grid	No reference
SN 2018dej	21:09:46.14	-50:14:12.41	0.058	In MSIP grid	No reference
SN 2018dei	13:23:43.12	-25:24:32.33	0.041	In MSIP grid	No reference
SN 2018ddy	22:59:57.34	-45:25:53.33	0.051	In MSIP grid	No reference
SN 2018dds	17:44:18.15	+68:01:44.66	0.075	In MSIP grid	Detectable g+R
SN 2018ddi	03:39:35.12	-06:19:30.29	0.021	In MSIP grid	No reference
SN 2018ddh	12:18:44.04	+44:46:55.11	0.038	In MSIP grid	Detectable g+R
SN 2018ddg	14:12:18.25	+62:38:34.72	0.073	In MSIP grid	Detectable g+R
SN 2018ddb	00:02:49.71	-66:11:06.14	0.029	In MSIP grid	No reference
SN 2018dda	22:08:14.15	-25:03:41.58	0.018	In MSIP grid	No reference
SN 2018dcn	17:06:44.02	+18:21:25.41	0.050	In MSIP grid	Detectable g or R
SN 2018dcm	17:25:41.47	+23:52:08.96	0.064	In MSIP grid	Detectable g+R
SN 2018dbe	14:27:55.24	+40:58:27.64	0.087	In MSIP grid	Detectable g+R
SN 2018dbd	16:52:47.35	+51:33:48.34	0.075	In MSIP grid	Detectable g+R
SN 2018dbc	15:21:24.31	+69:36:22.63	0.080	In MSIP grid	Detectable g+R
SN 2018cxm	14:53:58.33	+26:00:07.09	0.048	In MSIP grid	Detectable g+R
SN 2018cxl	17:44:24.63	+55:10:31.56	0.060	In MSIP grid	Detectable g+R
SN 2018cxj	12:46:30.22	+77:16:51.51	0.050	In MSIP grid	Detectable g or R
SN 2018cxe	17:21:01.63	+26:09:07.31	0.044	Outside MSIP grid	Not observable
SN 2018cvx	12:51:27.49	+20:36:23.29	0.062	In MSIP grid	Detectable g+R
SN 2018cvw	15:57:02.31	+37:25:01.84	0.031	In MSIP grid	Detectable g+R
SN 2018cvv	12:04:35.87	+12:33:24.45	0.065	In MSIP grid	Detectable g or R
SN 2018cvu	13:15:34.32	+28:20:34.48	0.102	In MSIP grid	Detectable g+R
SN 2018cvt	14:51:53.63	+46:38:44.70	0.074	In MSIP grid	Detectable g+R
SN 2018cvs	13:41:07.97	+28:53:11.47	0.105	In MSIP grid	Detectable g+R
SN 2018cvr	14:45:24.55	+78:17:05.00	0.100	Chip / RC border	Not clear
SN 2018cvq	15:52:54.43	+50:37:10.10	0.067	In MSIP grid	Detectable g+R
SN 2018cvh	15:07:58.60	+01:13:56.63	0.035	In MSIP grid	No reference
SN 2018cvf	12:06:40.62	+59:30:48.11	0.064	In MSIP grid	Detectable g+R
SN 2018cvd	13:14:40.26	+24:00:20.68	0.067	In MSIP grid	Detectable g+R
SN 2018cuw	18:46:14.38	+35:58:07.27	0.024	In MSIP grid	Detectable g+R
SN 2018cua	15:32:03.56	+23:31:01.33	0.091	In MSIP grid	Detectable g+R
SN 2018cty	13:01:45.70	+61:27:55.73	0.056	In MSIP grid	Detectable g+R
SN 2018cts	13:59:14.00	+28:32:26.76	0.064	In MSIP grid	Detectable g or R
SN 2018ctq	12:13:47.91	+40:42:56.35	0.100	In MSIP grid	Detectable g+R
SN 2018cto	17:24:32.04	+70:22:20.81	0.051	In MSIP grid	Detectable g+R
SN 2018ctm	18:26:14.18	+45:00:36.69	0.065	In MSIP grid	Detectable g+R
SN 2018cti	22:17:30.73	+11:43:17.58	0.035	Outside MSIP grid	Not observable
SN 2018ctc	14:18:18.02	+28:58:23.88	0.042	In MSIP grid	Detectable g or R
SN 2018ctb	22:01:08.36	+20:03:05.29	0.029	In MSIP grid	No reference
SN 2018crs	17:20:24.40	+55:12:52.72	0.072	In MSIP grid	Detectable g+R
SN 2018crr	16:59:37.23	+59:04:23.73	0.073	In MSIP grid	Detectable g+R
SN 2018cro	21:00:49.26	+09:31:28.18	0.076	In MSIP grid	No reference
SN 2018crn	18:55:21.84	+56:35:18.14	0.050	In MSIP grid	Detectable g+R
SN 2018crj	17:58:02.75	+69:04:22.13	0.088	In MSIP grid	Detectable g+R
SN 2018cri	16:11:21.47	+36:59:39.41	0.064	In MSIP grid	Detectable g+R
SN 2018cqw	18:17:32.21	+19:26:40.49	nan	Outside MSIP grid	Not observable
SN 2018cqv	23:18:28.71	-25:59:25.38	0.103	In MSIP grid	No reference
SN 2018cqj	09:40:21.46	-06:59:19.76	0.021	In MSIP grid	No reference
SN 2018cqa	14:47:45.78	+32:45:06.80	0.060	Outside MSIP grid	Not observable
SN 2018coy	20:20:28.88	-33:23:37.00	0.039	Outside MSIP grid	Not observable
SN 2018cov	23:49:48.24	-14:07:09.95	0.051	In MSIP grid	No reference
SN 2018coj	12:01:54.86	+36:53:42.71	0.079	In MSIP grid	Detectable g or R

Name	RA	DEC	Redshift	ZTF field match	Detectable
SN 2018coi	16:18:57.98	+56:43:00.77	0.059	In MSIP grid	Detectable g+R
SN 2018coh	17:20:38.66	+52:02:30.97	0.085	In MSIP grid	Detectable g+R
SN 2018cof	14:59:54.39	+39:04:43.78	0.092	In MSIP grid	Detectable g+R
SN 2018coe	16:51:37.37	+61:32:43.34	0.080	In MSIP grid	Detectable g+R
SN 2018cod	13:20:27.96	+62:18:03.02	0.030	In MSIP grid	Detectable g+R
SN 2018coc	16:38:32.00	+05:07:35.30	0.090	In MSIP grid	Detectable g or R
SN 2018cny	15:04:16.62	+35:48:54.11	0.047	In MSIP grid	Detectable g+R
SN 2018cnu	02:10:02.21	+37:02:18.31	0.025	In MSIP grid	No reference
SN 2018cnp	13:49:39.47	+47:49:09.37	0.028	Outside MSIP grid	Not observable
SN 2018cno	02:10:32.76	-06:52:27.37	0.043	In MSIP grid	No reference
SN 2018cng	15:45:29.05	+35:51:19.09	0.066	In MSIP grid	Detectable g+R
SN 2018cne	16:18:42.70	+40:04:20.83	0.080	In MSIP grid	Detectable g+R
SN 2018cmu	09:17:59.90	+50:00:07.81	0.034	In MSIP grid	Detectable g or R
SN 2018cmt	23:56:55.72	-24:59:47.58	0.074	In MSIP grid	No reference
SN 2018cmo	23:14:22.23	-02:02:01.86	0.026	In MSIP grid	No reference
SN 2018cmk	11:38:29.86	+20:31:44.26	nan	In MSIP grid	Detectable g or R
SN 2018cjy	12:59:45.30	-25:36:06.13	0.064	In MSIP grid	No reference
SN 2018cjw	17:46:41.41	+27:35:22.93	0.094	In MSIP grid	Detectable g+R
SN 2018cjn	18:46:20.42	+70:44:13.46	0.100	In MSIP grid	Detectable g or R
SN 2018cjg	13:31:55.35	+23:16:59.85	0.045	In MSIP grid	Detectable g or R
SN 2018cjd	14:58:20.02	-37:33:25.16	0.026	In MSIP grid	No reference
SN 2018cif	22:03:00.93	+02:35:51.31	0.029	Outside MSIP grid	Not observable
SN 2018cfa	16:49:39.12	+45:29:32.64	0.030	In MSIP grid	Detectable g+R